Inorganic Chemistry

Article

Methanolysis and Phenolysis Routes to Fe₆, Fe₈, and Fe₁₀ Complexes and Their Magnetic Properties: A New Type of Fe₈ Ferric Wheel

Cristina Cañada-Vilalta,[†] Ted A. O'Brien,[†,‡] Maren Pink,[†] Ernest R. Davidson,[†,§] and George Christou*,[†,∥]

Department of Chemistry and the Molecular Structure Center, Indiana University, Bloomington, Indiana 47405-7102, and Department of Chemistry, University of Florida, Gainesville, Florida 32611-7200

Alcoholysis of preformed tetranuclear and hexanuclear iron(III) clusters has been employed for the synthesis of four higher-nuclearity clusters. Treatment of $[Fe_4O_2(O_2CMe)_7(bpy)_2](ClO_4)$ with phenol affords the hexanuclear cluster $[Fe_6O_3(O_2CMe)_9(OPh)_2(bpy)_2](ClO_4)$ (**1**). Reaction of $[Fe_6O_2(OH)_2(O_2CR)_{10}(hep)_2]$ (R = Bu^t or Ph) with PhOH affords the new "ferric wheel" complexes $[Fe_8(OH)_4(OPh)_8(O_2CR)_{12}]$ [R = Bu^t (**2**) or Ph (**3**)]. Complexes **2** and **3** exhibit the same structure, which is an unprecedented type for Fe(III). In contrast, treatment of $[Fe_6O_2(OH)_2(O_2CBu^t)_{10}(hep)_2]$ with MeOH leads to the formation of $[Fe_{10}(OMe)_{20}(O_2CBu^t)_{10}]$ (**4**), which exhibits the more common type of ferric wheel seen in analogous complexes with other carboxylate groups. Solid-state variable-temperature magnetic susceptibility measurements indicate spin-singlet ground states for complexes **2** and **4**. The recently developed semiempirical method ZILSH was used to estimate the pairwise exchange parameters (J_{AB}) and the average spin couplings $\hat{S}_A \cdot \hat{S}_B$ between the Fe(III) centers, providing a clear depiction of the overall magnetic behavior of the molecules. All exchange interactions between adjacent Fe(III) atoms are antiferromagnetic.

Introduction

Iron plays an important role in diverse areas of nature, from mineralogy to biology. Its most common oxidation state is 3+, which is found in oxide-based minerals such as hematite or ferrihydrite,[11] as well as in a number of biological systems. Of particular interest is the biomineralization of the element and its deposition into iron storage proteins. In most living organisms, iron is stored in the protein ferritin, which can contain up to ca. 4500 Fe(III) ions in a polymeric oxo-hydroxo lattice.[2] Amino acid side-chain carboxylate residues are believed to have a key function as binding sites for the incorporation of the metal. Polynuclear iron clusters contain-ing carboxylate as well as oxide, hydroxide, and/or alkoxide ligands have therefore been pursued as inorganic models for this system and for the biomineralization process in general.

Another aspect that makes the study of polynuclear iron complexes especially appealing is their potential to display interesting magnetic properties. Although interactions between Fe(III) ions are generally antiferromagnetic, some clusters experience spin frustration or display particular Fe$_x$ topological arrangements that can result in ground states with reasonably large spins. In favorable cases where these large spin ground states are coupled with a significant magnetic anisotropy, the compounds can behave as single-molecule magnets. This is the case for $[Fe_4(OMe)_6(dpm)_6]$[3] and $[Fe_8O_2(OH)_{12}(tacn)_6]^{8+}$,[4,5] among others.

For the above reasons, there is much interest in developing synthetic procedures to new polynuclear iron compounds.

* To whom correspondence should be addressed. E-mail: christou@chem.ufl.edu.
† Indiana University.
‡ Present address: Department of Chemistry, Indiana University−Purdue University Indianapolis, Indianapolis, IN 46202-3274.
§ Present address: Department of Chemistry, University of Washington, Seattle, WA 98195-1700.
∥ University of Florida.
(1) (a) Zachara, J. M.; Kukkadapu, R. K.; Fredrickson, J. K.; Gorby, Y. A.; Smith, S. C. *Geomicrobiol. J.* **2002**, *19*, 179. (b) Zachara, J. M.; Fredrickson, J.; Smith, S. C.; Kukkadapu, R. K. *Abstr. Pap.−Am. Chem. Soc. 220th ENVR* **2000**, 195. (c) Brown, D. A.; Sherriff, B. L.; Sawicki, J. A.; Sparling, R. *Geochim. Cosmochim. Acta* **1999**, *63*, 2163.

(2) (a) Theil, E. C. *Annu. Rev. Biochem.* **1987**, *57*, 289 and references therein. (b) Xu, B.; Chasteen, N. D. *J. Biol. Chem.* **1991**, *266*, 19965. (c) Grant, R. A.; Filman, D. J.; Finkel, S. E.; Kolter, R.; Hogle, J. M. *Nat. Struct. Biol.* **1998**, *5*, 294.
(3) Barra, A. L.; Caneschi, A.; Cornia, A.; Fabrizi de Biani, F.; Gatteschi, D.; Sangregorio, C.; Sessoli R.; Sorace, L. *J. Am. Chem. Soc.* **1999**, *121*, 5302.
(4) Wieghardt, K.; Pohl, K.; Jibril, I.; Huttner, G. *Angew. Chem., Int. Ed. Engl.* **1984**, *23*, 77.

Hydrolysis of iron salts in the presence of carboxylate groups, with or without other chelating ligands, has proven to be a very useful method for obtaining both oxide- and hydroxide-containing clusters. This approach has resulted in a number of compounds with diverse nuclearities and Fe_x topological arrangements, such as $[Fe_8O_2(OH)_{12}(tacn)_6]^{8+}$,[5] $[Fe_{11}O_6(OH)_6$-$(O_2CPh)_{15}]$,[6] and $[Fe_{19}O_6(OH)_{14}(heidi)_{10}(H_2O)_{12}]^+$ [H_3heidi $= N(CH_2COOH)_2(CH_2CH_2OH)]$.[7]

A very common approach for obtaining alkoxide-containing compounds has been the metathesis reaction between iron salts and metal alkoxides. Some examples include the use of lithium methoxide for the synthesis of the iron alkoxide cube $[Fe_4(OMe)_5(MeOH)_3(O_2CPh)_4]$,[8] potassium or cesium methoxide for the preparation of $[Fe(OMe)_2(dbm)]_{12}$,[9] and sodium ethoxide for the preparation of $[Fe_9O_3(OEt)_{21}]$.[10] Very recently, a similar reaction was reported that employed aluminum alkoxides in a reaction with a preformed cluster rather than a simple iron salt. In this way, $[Fe_4O_2(O_2CPh)_8$-$(py)_2]$ was converted with $Al(OR)_3$ ($R = Pr^i$, Bu) to the hexanuclear product $[Fe_6O_2(OR)_8(O_2CPh)_6]$.[11]

A related method uses the relative acidity of alcohols to transform iron(III) salts or (more rarely) preformed Fe_x clusters into alkoxide-containing complexes in the absence of more aggressive alkoxide sources. These controlled alcoholysis reactions take place under milder conditions than the aforementioned metathesis reactions. Complexes obtained in this way include $[Fe_6O_2(OMe)_{12}(tren)_2]^{2+}$,[12] $[Fe_{10}(OMe)_{20}(O_2$-$CCH_2Cl)_{10}]$,[13] $[Fe_8O_4(L)_2(O_2CPh)_{14}(HL)_2]$ (HL = neopen-tanol),[14] and $[Fe_6O_3(O_2CMe)_9(OEt)_2(bpy)_2]^+$.[15] In these reactions, the treatment with an alcohol triggered the aggregation of small units into products with higher nuclearities.

The work presented here continues this last approach, using preformed Fe_4 and Fe_6 compounds as starting materials. We have also explored for the first time the use of the aromatic alcohol PhOH in such reactions and compared the products obtained from a given alcoholysis reaction when the alcohol is either MeOH or PhOH. PhOH was chosen primarily because of its relative bulkiness and acidity ($pK_a = 9.98$ vs 15.5 for MeOH). The latter property makes PhOH

an attractive reagent, because an early step in the alcoholysis reaction of Fe_x clusters likely involves proton transfer from the alcohol to a bound ligand. Although phenol is a widely used substance, there are very few examples of phenoxide as a ligand in iron chemistry. For example, the only crystallographically characterized compounds containing Fe-bound phenoxide groups are a small number of iron−sulfur clusters[16] and two porphyrin-based mononuclear com-pounds.[17]

The reactions described in this report between methanol or PhOH and polynuclear iron starting materials with metal nuclearities of 4 and 6 have afforded four new complexes with nuclearities of 6, 8, and 10. We describe the syntheses, structures, and magnetic properties of these new compounds, as well as our conclusions about the impact of the MeOH vs PhOH difference on the reaction products.

Experimental Section

Syntheses. All reactions were performed under aerobic condi-tions. Solvents and reagents were obtained from commercial sources and used as received. $[Fe_4O_2(O_2CMe)_7(bpy)_2](ClO_4)$,[18] $[Fe_6O_2(OH)_2$-$(O_2CBu^t)_{10}(hep)_2]$,[19] and $[Fe_6O_2(OH)_2(O_2CPh)_{10}(hep)_2]$[20] were pre-pared as described elsewhere.

$[Fe_6O_3(O_2CMe)_9(OPh)_2(bpy)_2](ClO_4)$ (1). A dark green solution of $[Fe_4O_2(O_2CMe)_7(bpy)_2](ClO_4)$ (0.35 g, 0.32 mmol) in MeCN (12 mL) was treated with a large excess of PhOH (0. 35 g, 3.7 mmol). The resulting mixture was filtered and allowed to stand undisturbed for several days. The color of the solution gradually changed to red-purple, and after concentration by slow evaporation, small, deeply colored red-purple crystals of $1 \cdot 2MeCN \cdot PhOH$ were obtained. These crystals were separated from the mother solution by filtration, washed copiously with hexanes to remove excess PhOH, and dried in air. The yield was 35%. The compound was identified by X-ray crystallography as structurally analogous with $[Fe_6O_3(O_2CMe)_9(OEt)_2(bpy)_2]^{+ 15}$ and was therefore not character-ized or studied further.

$[Fe_8(OH)_4(OPh)_8(O_2CBu^t)_{12}]$ (2). A solution of $[Fe_6O_2(OH)_2(O_2$-$CBu^t)_{10}(hep)_2]$ (0.45 g, 0.27 mmol) in CH_2Cl_2 (10 mL) was treated with a large excess of PhOH (0.46 g, 4.8 mmol). The resulting, very dark red solution was stirred for 10 min and filtered, and the filtrate was left undisturbed in a sealed flask. Dark red crystals of $2 \cdot H_2O \cdot CH_2Cl_2$ slowly formed over 2 days, and they were isolated by filtration, washed with hexanes, and dried in air. The yield was 60%. Vacuum-dried solid analyzed as solvent-free. Anal. Calcd (found) for $C_{108}H_{152}Fe_8O_{36}$: C, 52.45 (52.55); H, 6.19 (6.36)%.

$[Fe_8(OH)_4(OPh)_8(O_2CPh)_{12}]$ (3). A solution of $[Fe_6O_2(OH)_2(O_2$-$CPh)_{10}(hep)_2]$ (0.36 g, 0.20 mmol) in $CHCl_3$ was treated with a

(5) (a) Delfs, C.; Gatteschi, D.; Pardi, L.; Sessoli, R.; Wieghardt K.; Hanke, D. *Inorg. Chem.* **1993**, *32*, 3099. (b) Wernsdorfer, W. *Adv. Chem. Phys.* **2001**, *118*, 99. (c) Furukawa, Y.; Aizawa, K.; Kumagai, K.-I.; Lascialfari, A.; Aldrovandi, S.; Borsa, F.; Sessoli, R.; Gatteschi, D. *Mol. Cryst. Liq. Cryst. A* **2002**, *379*, 191.

(6) Gorun, S. M.; Papaefthymiou, G. C.; Frankel, R. B.; Lippard, S. J. *J. Am. Chem. Soc.* **1987**, *109*, 3337.

(7) (a) Goodwind, J. C.; Sessoli, R.; Gatteschi, D.; Wernsdorfer, W.; Powell, A. K.; Heath, S. L. *J. Chem. Soc., Dalton Trans.* **2000**. (b) Powell, A. K.; Heath, S. L.; Gatteschi, D.; Pardi, L.; Sessoli, R.; Spina, G.; Del Giallo, F.; Pieralli, F. *J. Am. Chem. Soc.* **1995**, *117*, 2491.

(8) Taft, K. L.; Caneschi, A.; Pence, L. E.; Delfs, C. D.; Papaefthymiou, G. C.; Lippard, S. J. *J. Am. Chem. Soc.* **1993**, *115*, 11753.

(9) Abbati, G. L.; Caneschi, A.; Cornia, A.; Fabretti, A. C.; Gatteschi, D. *Inorg. Chim. Acta* **2000**, *297* (1−2), 291.

(10) Veith, M.; Gratz, F.; Huch, V. *Eur. J. Inorg. Chem.* **2001**, *2*, 367.

(11) Ammala, P. S.; Batten, S. R.; Cashion, J. D.; Kepert, C. M.; Moubaraki, B.; Murray, K. S.; Spiccia, L.; West, B. O. *Inorg. Chim. Acta* **2002**, *331*, 90.

(12) Nair, V. S.; Hagen, K. S. *Inorg. Chem.* **1992**, *31*, 4048.

(13) Taft, K. L.; Lippard, S. J. *J. Am. Chem. Soc.* **1990**, *112*, 9629.

(14) Ammala, P.; Cashion, J. D.; Kepert, C. M.; Moubaraki, B.; Murray, K. S.; Spiccia, L.; West, B. O. *Angew. Chem., Int. Ed. Engl.* **2000**, *39*, 1688.

(15) Seddon, E. J.; Huffman, J. C.; Christou, G. *J. Chem. Soc., Dalton Trans.* **2000**, *23*, 4446.

(16) (a) Teo, B. K.; Antonio, M. R.; Tieckelmann, R. H.; Silvis, H. C.; Averill, B. A. *J. Am. Chem. Soc.* **1982**, *104*, 6126. (b) Cleland, W. E.; Holtman, D. A.; Sabat, M.; Ibers, James A.; DeFotis, G. C.; Averill, B. A. *J. Am. Chem. Soc.* **1983**, *105*, 6021. (c) Kanatzidis, M. G.; Baenziger, N. C.; Coucouvanis, D.; Simopoulos, A.; Kostikas, A. *J. Am. Chem. Soc.* **1984**, *106*, 4500.

(17) (a) Nasri, H.; Fischer, J.; Weiss, R.; Bill, E.; Trautwein, A. *J. Am. Chem. Soc.* **1987**, *109*, 2549. (b) Byrn, M. P.; Curtis, C. J.; Hsiou, Y.; Khan, S. I.; Sawin, P. A.; Tendick, S. K.; Terzis, A.; Strouse, C. E. *J. Am. Chem. Soc.* **1993**, *115*, 9480.

(18) McCusker, J. K.; Vincent, J. B.; Schmitt, E. A.; Mino, M. L.; Shin, K. Coggin, D. K.; Hagen, P. M.; Huffman, J. C.; Christou, G.; Hendrickson, D. N. *J. Am. Chem. Soc.* **1991**, *113*, 3012.

(19) Cañada-Vilalta, C.; Rumberger, E.; Brechin, E.; Wernsdorfer, W.; Folting, K.; Davidson, E. R.; Hendrickson, D. N.; Christou, G. *J. Chem. Soc., Dalton Trans.* **2002**, *21*, 4005.

(20) Cañada-Vilalta, C.; O'Brien, T. A.; Pink, M.; Davidson, E. R.; Christou, G., manuscript submitted.

Table 1. Crystallographic Data for **1**·2MeCN·PhOH, **2**·H₂O·CH₂Cl₂, **3**·H₂O·3CHCl₃, and **4**·CHCl₃

	1·2MeCN·PhOH	**2**·H₂O·CH₂Cl₂	**3**·H₂O·3CHCl₃	**4**·CHCl₃
empirical formula	$C_{60}H_{65}ClFe_6N_6O_{28}$	$C_{109}H_{156}Cl_2Fe_8O_{37}$	$C_{135}H_{109}Cl_9Fe_8O_{37}$	$C_{71}H_{151}Cl_3Fe_{10}O_{40}$
formula weight	1688.73	2576.04	3089.07	2309.77
crystal color, size (mm³)	red, 0.18 × 0.18 × 0.10	red, 0.26 × 0.18 × 0.10	red, 0.10 × 0.03 × 0.02	yellow, 0.22 × 0.21 × 0.17
temperature (K)	120(2)	120(2)	120(2)	173(2)
wavelength (Å)	0.710 73	0.710 73	0.710 73	0.710 73
crystal system, space group	monoclinic, $P2_1/n$	monoclinic, $P2_1/n$	monoclinic, $P2_1/c$	triclinic, $P\bar{1}$(bar)
unit cell dimensions	$a = 21.1897(9)$ Å	$a = 16.2537(7)$ Å	$a = 13.330(2)$ Å	$a = 18.940(1)$ Å
	$\alpha = 90°$	$\alpha = 90°$	$\alpha = 90°$	$\alpha = 112.896(1)°$
	$b = 14.9275(6)$ Å	$b = 19.1441(8)$ Å	$b = 21.096(3)$ Å	$b = 19.054(1)$ Å
	$\beta = 105.171(1)°$	$\beta = 103.523(1)°$	$\beta = 100.780(3)°$	$\beta = 102.991(1)°$
	$c = 23.196(1)$ Å	$c = 21.4339(9)$ Å	$c = 25.189(3)$ Å	$c = 19.096(1)$ Å
	$\gamma = 90°$	$\gamma = 90°$	$\gamma = 90°$	$\gamma = 109.123(1)°$
volume (Å³)	7081.5(5)	6484.5(5)	6958(2)	5485.1(5)
Z	4	2	2	2
density (calculated) (g/cm³)	1.584	1.319	1.474	1.399
absorption coefficient	1.320	0.982	1.059	1.427
absorption correction	semiempirical from equivalents	semiempirical from equivalents	semiempirical from equivalents	semiempirical from equivalents
data/parameters	20 687/128/961	13 247/237/935	12 328/18/869	32 002/33/1203
GOF[a]	1.018	1.049	0.995	1.021
final R indices[b,c] (observed data)	R = 10.0459, wR2 = 0.1243	R = 10.0523, wR2 = 0.1380	R = 10.0860, wR2 = 0.2068	R = 10.0417, wR2 = 0.1047
R indices[b,c] (all data)	R = 10.0707, wR2 = 0.140	R = 10.0644, wR2 = 0.1482	R = 10.1899, wR2 = 0.2613	R = 10.0812, wR2 = 0.1303
largest diff. peak and hole (e·Å⁻³)	1.491 and −1.162	1.320 and −0.822	1.599 and −1.047	1.135 and −0.784

[a] Goodness of fit = $[\sum[w(F_o^2 - F_c^2)^2]/N_{observations} - N_{parameters})]^{1/2}$, all data. [b] R1 = $\sum(|F_o| - |F_c|)/\sum|F_o|$. [c] wR2 = $\{\sum[w(F_o^2 - F_c^2)^2]/\sum[w(F_o^2)^2]\}^{1/2}$.

large excess of PhOH (2.0 g, 21 mmol). The resulting very dark green solution was stirred overnight and filtered. The filtrate was allowed to slowly evaporate, and the color changed to deep red over a period of several days. Very small, deep red needles of **3**·H₂O·3CHCl₃ were obtained in ~30% yield. The material was identified by X-ray crystallography as structurally analogous with **2** and was therefore not characterized or studied further.

[Fe₁₀(OMe)₂₀ (O₂CBuᵗ)₁₀] (4). [Fe₆O₂(OH)₂(O₂CBuᵗ)₁₀(hep)₂] (0.25 g, 0.15 mmol) was dissolved in CHCl₃ (10 mL), and the solution was filtered to remove a little undissolved product. MeOH (3 mL) was added to the solution, and the mixture was left undisturbed. A cloudy precipitate was observed after the first day, and dark yellow rhomboidal crystals of **4**·CHCl₃ formed after several weeks. They were collected by filtration, washed with hexanes, and dried in air. The yield was 13%. Vacuum-dried solid analyzed as solvent-free. Anal. Calcd (found) for C₇₀H₁₅₀Fe₁₀O₄₀: C, 38.38 (38.14); H, 6.90 (6.83)%.

X-ray Crystallography and Structure Solution. Data were collected using a Bruker SMART 6000 system. Suitable crystals were placed onto the tip of a 0.1-mm-diameter glass capillary and mounted on the goniostat. Data collection was carried out using Mo Kα radiation (graphite monochromator) with a detector distance of 5.0 cm. The intensity data were corrected for absorption (SADABS).[21a] Final cell constants were calculated from the *xyz* centroids of strong reflections after integration (SAINT).[21b] The space groups were determined on the basis of systematic absences and intensity statistics. The structures were solved by direct methods (SIR-92[22]) and refined by full-matrix least-squares (SHELXL-97[23]). All non-hydrogen atoms were refined with anisotropic displacement

parameters unless stated otherwise. The hydrogen atoms were placed in ideal positions and refined as riding atoms with relative isotropic displacement parameters. Crystallographic data collection and structure refinement details are listed in Table 1.

Compound **1**·2MeCN·PhOH crystallizes in the monoclinic space group $P2_1/n$ with an Fe₆ cation in a general position. One MeCN molecule and the perchlorate anion are disordered over two positions with different occupancies, and the second MeCN molecule is disordered over three positions. The PhOH is also disordered, but attempts to model the disorder failed through lack of convergence upon refinement. Therefore, the PhOH molecule was refined at one site and consequently displays relatively large displacement parameters.

Compound **2**·H₂O·CH₂Cl₂ crystallizes in the monoclinic space group $P2_1/n$. All non-hydrogen atoms were refined with anisotropic displacement parameters except for the CH₂Cl₂ molecule, which was refined isotropically. The structure contains numerous disordered groups. The phenoxide ligands display a correlated disorder: there are two possible arrangements for each set of four ligands on either side of the Fe₈ ring plane, which are disposed in a pinwheel fashion either clockwise or counterclockwise, with almost equal occupation factors (53:47%).

In addition, three of the carboxylate groups are each disordered over two positions with different occupancies. The CH₂Cl₂ molecule is disordered over at least two positions, with electron density in its vicinity indicating that additional sites might be occupied with low occupancies. Finally, the water molecule is disordered between two positions with equal weight, above and below the Fe₈ plane, and is involved in hydrogen bonding with the neighboring hydroxide groups. Another crystal of the same compound was also solved, and this crystallizes in the tetragonal group *I*4/*m*. In this case, there are no organic solvent molecules in the lattice, but there are two additional water molecules disordered over four sites. This confers 4-fold symmetry to the crystal. Both crystals can be described as polymorphs, in the broader sense of the term, given that the

(21) (a) Blessing, R. *Acta Crystallogr.* **1995**, *A51*, 33. (b) *SAINT 6.1*, Bruker Analytical X-ray Systems: Madison, WI, 1999.
(22) Altomare, A.; Cascarno, G.; Giacovazzo, C.; Gualardi, A.; *J. Appl. Cryst.* **1993**, *26*, 343.
(23) *SHELXTL-Plus V5.10*; Bruker Analytical X-ray Systems: Madison, WI, 1997.

compound is essentially the same except for the minimal solvent difference.

Compound $3 \cdot H_2O \cdot 3CHCl_3$ crystallizes in monoclinic space group $P2_1/c$. The small size of the crystal resulted in weak data, which explains the low data-to-parameter ratio. All non-hydrogen atoms except C2S in one of the lattice $CHCl_3$ molecules were refined with anisotropic thermal parameters. This chloroform molecule was refined with a set of restraints and a fixed site occupancy of 0.50. The relatively high R values were due to icing problems during the data collection. In contrast to the structure of complex 2, there is no disorder affecting the phenoxide groups of 3, and the phenyl rings were clearly located in a single conformation.

Compound $4 \cdot CHCl_3$ crystallizes in the triclinic space group $P\bar{1}$. All non-hydrogen atoms were refined with anisotropic thermal parameters. Some disorder was observed in two of the methoxide and two of the carboxylate groups. The complex packs inefficiently, leaving large voids of 156 Å^3 per unit cell in the structure, with no significant electron density within them.

Final values of the refinement discrepancy indices are listed in Table 1.

Computational Studies. Semiempirical unrestricted Hartree–Fock (UHF) molecular orbital calculations on 2 and 4 were carried out using the recently developed ZILSH method.[24,25] Several useful quantities are obtained from these calculations, including the spin couplings $\hat{S}_A \cdot \hat{S}_B$, exchange constants J_{AB}, and number of unpaired electrons per radical center (calculated as the sum of orbital spin densities for the center).[24] The ZILSH method has been successfully applied to 18 polynuclear[24,25a,c] and 65 dinuclear[25b] Fe(III) complexes. In cases where the Heisenberg Hamiltonian can be diagonalized readily (typically complexes with six or fewer metal atoms), the exchange constants can be refined to quantitatively fit variable-temperature magnetic susceptibility data. For larger cases, such as those considered in this paper, the method gives a qualitatively accurate description of the magnetic interactions, and correctly predicts the spin of the ground state in each case.[24,25]

Other Studies. Infrared spectra were recorded in the solid state (KBr pellets) on a Nicolet model 510P FTIR spectrophotometer in the 4000–400 cm^{-1} range. Elemental analyses (C, H, and N) were obtained on a Perkin-Elmer 2400 Series II apparatus. Magnetic susceptibility measurements were performed at Indiana University on a Quantum Design MPMS-XL SQUID magnetometer equipped with a 7-T magnet. Pascal's constants were used to estimate the diamagnetic correction, which was subtracted from the experimental susceptibility to give the molar magnetic susceptibility (χ_M).

Results and Discussion

Syntheses. Previous work by Seddon et al.[15] was directed toward the study of the alcoholysis reactions of $[Fe_4O_2]^{2+}$ butterfly complexes as a potential route to interesting new species. In one reaction, the hexanuclear compound $[Fe_6O_3(O_2CMe)_9(OEt)_2(bpy)_2](ClO_4)$ was obtained in very low yield from a concentrated ethanolic solution of $[Fe_4O_2(O_2CMe)_7(bpy)_2](ClO_4)$. This solution also afforded large quantities of $[Fe(bpy)_3](ClO_4)_2$ in a complex reaction in which a number of additional Fe-containing species were believed to coexist

in solution. The same type of transformation was explored in the present work using PhOH as the alcohol and a very concentrated MeCN solution of $[Fe_4O_2(O_2CMe)_7(bpy)_2]$-$(ClO_4)$. This resulted in a color change from dark green to red-purple over a period of several hours, and slow evaporation of the solvent led to isolation of $[Fe_6O_3(O_2CMe)_9(OPh)_2$-$(bpy)_2](ClO_4)$ (1). This complex was found to have a structure analogous to that of the ethoxide-containing derivative but with PhO^- in place of EtO^- groups. However, the yield of the Fe_6 complex was considerably higher in this case (35%), and the only limitation of the synthesis was the cocrystallization of excess PhOH as the solution became too concentrated. No clear evidence was found for $[Fe(bpy)_3]$-$(ClO_4)_2$ or any species other than 1. These observations suggest that the reaction is accurately summarized by eq 1, with the crystallization of the sparingly soluble product likely the main driving force toward formation of 1.

$$3[Fe_4O_2(O_2CMe)_7(bpy)_2]^+ + 4PhOH \rightarrow$$
$$2[Fe_6O_3(O_2CMe)_9(OPh)_2(bpy)_2]^+ + 2bpy + 3MeCO_2H +$$
$$H^+ \quad (1)$$
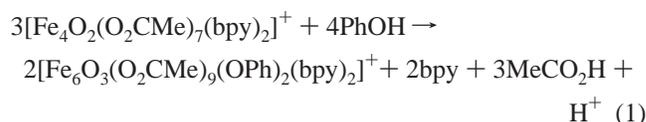
Although the main product of this phenolysis reaction in MeCN is essentially the same as that of the earlier ethanolysis reaction in EtOH, the number of isolated products is reduced, possibly because of the greater solubility of coproducts in MeCN compared to EtOH. The formation and presence of some $[Fe(bpy)_3]^+$ in the reaction solution cannot be ruled out.

We have recently reported several new hexanuclear iron species with oxide, hydroxide, and carboxylate ligation.[20] The possibility of obtaining larger-nuclearity compounds by alcohol-induced aggregation of these preformed species seemed very attractive, and therefore, their reactivities with different alcohols was explored. The initial results were obtained from the use of MeOH. $[Fe_6O_2(OH)_2(O_2CBu^t)_{10}$-$(hep)_2]$ is only sparingly soluble in MeOH, so it was first dissolved in $CHCl_3$ and treated with an excess of the alcohol. The resulting reaction produced a light yellow powder, as well as green crystals of the decanuclear wheel compound $[Fe_{10}(OMe)_{20}(O_2CBu^t)_{10}]$ (4), which could be readily separated from the powder. This transformation is summarized in eq 2, although the formation of yellow solid byproduct indicates that the reaction is more complicated.

$$5[Fe_6O_2(OH)_2(O_2CBu^t)_{10}(hep)_2] + 60MeOH \rightarrow$$
$$3[Fe_{10}(OMe)_{20}(O_2CBu^t)_{10}] + 20H_2O + 10hepH +$$
$$20Bu^tCO_2H \quad (2)$$
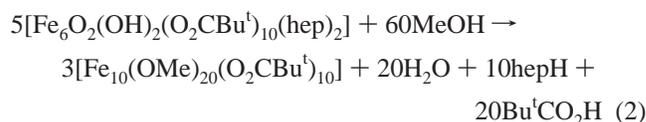
Compound 4 is another member of the growing family of Fe_{10} "ferric wheels" of general formula $[Fe_{10}(OMe)_{20}(O_2$-$CR)_{10}]$, of which several examples are now known differing in the carboxylate R groups.[26–29]
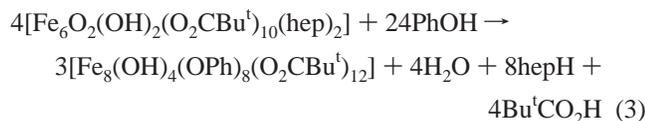
(24) O'Brien, T. A.; Davidson, E. R. *Int. J. Quantum Chem.* **2003**, *92*, 294.

(25) (a) O'Brien, T. A.; Cañada-Vilalta, C.; Christou, G.; Davidson, E. R. *J. Phys. Chem. A*, manuscript submitted. (b) O'Brien, T. A.; Cañada-Vilalta, C.; Davidson, E. R. *J. Comput. Chem.*, manuscript in preparation. (c) Cañada-Vilalta, C.; O'Brien, T. A.; Pink, M.; Davidson, E. R.; Christou, G., manuscript submitted.

(26) Kooijman, H.; Spek, A. L.; Bouwman, E.; Micciche, F.; Warzeska, S. T.; Reedijk, J. *Acta Cryst. E: Struct. Rep. Online* **2002**, *E58*, m93.

(27) Benelli, C.; Parsons, S.; Solan, G. A.; Winpenny, R. E. P. *Angew. Chem., Int. Ed. Engl.* **1996**, *35*, 1825.

Very different results were obtained when PhOH was used instead of MeOH. In the structure of compound **4** (vide infra), several of the methoxide groups are directed toward the center of the ring. This region of the molecule is too small to accommodate phenyl rather than methyl groups, and we therefore suspected that, if the phenolysis reaction also gave a wheel product, this product would likely have a structure distinctly different from that of **4**. This indeed turned out to be the case. Treatment of $[Fe_4O_2(O_2CMe)_7(bpy)_2](ClO_4)$ with an excess of PhOH in CH_2Cl_2 afforded the new compound $[Fe_8(OH)_4(OPh)_8(O_2CBu^t)_{12}]$ (**2**) in high yield ($\sim$60%). This is a wheel complex, but with a structure very different from that of **4** (vide infra). Its formation is summarized in eq 3. Note that, in both this reaction and that of eq 2, none of the hep⁻ chelate groups of the starting material are found in the product.

$$4[Fe_6O_2(OH)_2(O_2CBu^t)_{10}(hep)_2] + 24PhOH \rightarrow$$
$$3[Fe_8(OH)_4(OPh)_8(O_2CBu^t)_{12}] + 4H_2O + 8hepH +$$
$$4Bu^tCO_2H \quad (3)$$

In a similar fashion, treatment of the benzoate complex $[Fe_6O_2(OH)_2(O_2CPh)_{10}(hep)_2]$ with an excess of PhOH in $CHCl_3$ resulted in $[Fe_8(OH)_4(OPh)_8(O_2CPh)_{12}]$ (**3**), the benzoate analogue of complex **2**. In contrast, analogous reactions using 2-MeC_6H_4OH, $2,6\text{-Me}_2C_6H_3OH$, $2,6\text{-Bu}^t_2C_6H_3OH$, and $2,6\text{-Cl}_2C_6H_3OH$ did not lead to clean products that we could identify; the only isolated solid identified was Fe_6 starting material, which shows a great tendency to crystallize in a number of different polymorphs, often incorporating the added phenolic reagent in the lattice. The phenolysis reactions were also performed in the presence of different NBu^n_4X salts ($X = Cl^-$, Br^-, PF_6^-, ClO_4^-) with the aim of replacing the guest water molecule in the central cavity with a larger group, perhaps leading to the crystallization of a larger-size Fe_x wheel. However, in every case, the isolated product was complex **2** with a water molecule in the cavity.

Description of Structures. $Fe_6O_3(O_2CMe)_9(OPh)_2(bpy)_2$]-$(ClO_4)\cdot2MeCN\cdot PhOH$ ($1\cdot2MeCN\cdot PhOH$). This compound crystallizes in the monoclinic space group $P2_1/n$, with one Fe_6 cation, one perchlorate anion, one PhOH, and two MeCN molecules in the asymmetric unit. An ORTEP representation and stereoview of the cation of complex **1** are shown in Figure 1, and its $[Fe_6O_5]$ core is shown in Figure 2. Selected bond distances and angles are listed in Table 2, where corresponding values are also provided for the analogous ethoxide complex $[Fe_6O_3(O_2CMe)_9(OEt)_2(bpy)_2]^{+}$.[15]

The core of the cation of **1** can be described as two triangular oxide-centered $[Fe_3(\mu_3\text{-O})]^{7+}$ units connected together by μ_4-oxide ion O2, which bridges an Fe_2 edge in each of the two triangular units. The Fe–O distances involving O2 are all very similar and range between 2.004 and 2.029 Å. The geometry at O2 is distorted tetrahedral,
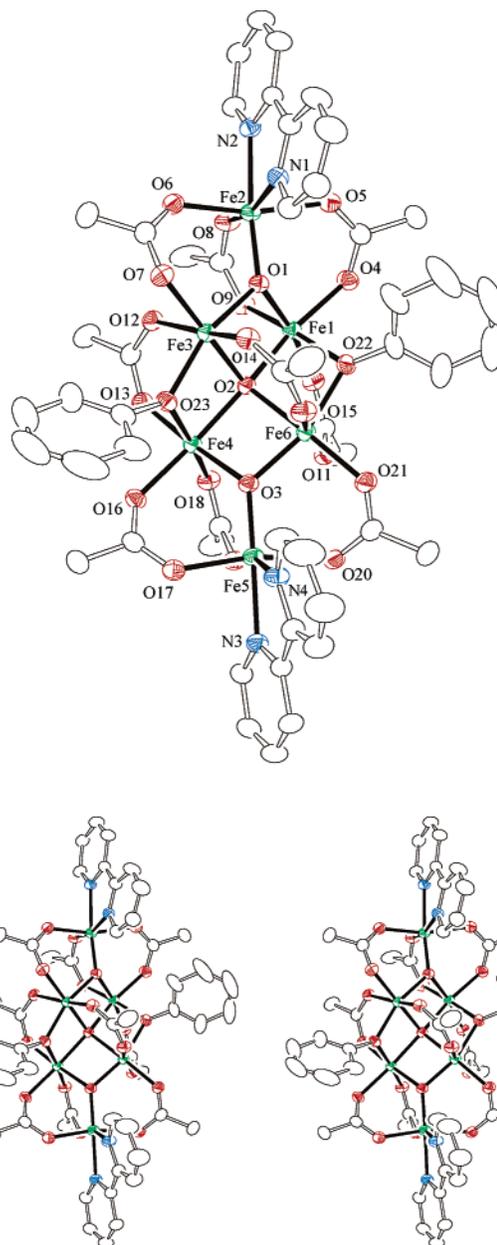
(28) Taft, K. L.; Delfs, C. D.; Papaefthymiou, G. C.; Foner, S.; Gatteschi, D.; Lippard, S. J. *J. Am. Chem. Soc.* **1994**, *116*, 823.

(29) Frey, M.; Harris, S. G.; Holmes, J. M.; Nation, D. A.; Parsons, S.; Tasker, P. A.; Teat, S. J.; Winpenny, R. E. P. *Angew. Chem., Int. Ed. Engl.* **1998**, *37*, 3246.
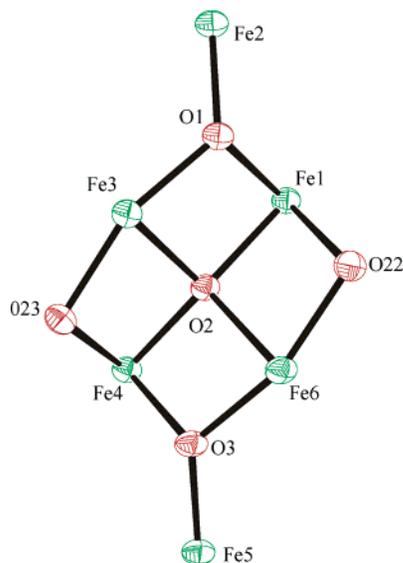
Figure 1. Labeled ORTEP representation and stereopair of the cation of complex **1** at the 50% probability level. Hydrogen atoms have been omitted for clarity.

and the two Fe_3 triangular units are thus essentially perpendicular, as best seen in the stereoview of Figure 1. The angles and bond lengths around the μ_3-oxide ions O1 and O3 are very asymmetrical. Their Fe–O bond lengths to the end Fe ions average 1.834 Å, whereas those to the body metal ions are longer, ranging from 1.925 to 1.949 Å. As expected, the distances around the μ_3-oxide ions are shorter than those around the μ_4-oxide ion. The Fe–O^{2-}–Fe angles within each triangular unit are also inequivalent: the angle involving two central Fe atoms, e.g., Fe1–O1–Fe3 [99.79(8)°], is significantly smaller than the angles involving central and end Fe atoms (average, 124.3°). The latter angle is also wider when there is only one carboxylate bridging the two metals, e.g., Fe2–O1–Fe3 [127.8(1)°] than when there are two bridging carboxylate groups, e.g., Fe1–O1–Fe2 [120.7(1)°]. Similar

Figure 2. Labeled ORTEP representation of the $[Fe_6O_5]^{8+}$ core of complex **1**.

Table 2. Comparison of Selected Bond Distances (Å) and Angles (deg) for the Cations $[Fe_6O_3(O_2CMe)_9(OR)_2(bpy)_2]^+$ [R = Ph (**1**), Et]

	R = Ph	R = Et		R = Ph	R = Et
Fe1−O1	1.9486(2)	1.948(2)	Fe2−O1−Fe3	127.8(1)	129.6(3)
Fe1−O2	2.024(2)	2.014(2)	Fe2−O1−Fe1	120.7(1)	120.4(3)
Fe1−O22	2.039(2)	1.999(2)	Fe3−O1−Fe1	99.79(8)	99.1(2)
Fe2−O1	1.8362(2)	1.841(2)	Fe4−O2−Fe3	98.70(8)	98.0(2)
Fe3−O1	1.933(2)	1.937(2)	Fe3−O2−Fe1	94.5(1)	94.0(2)
Fe3−O2	2.021(2)	2.028(2)	Fe4−O2−Fe6	94.24(8)	94.1(2)
Fe3−O23	2.003(2)	1.990(2)	Fe1−O2−Fe6	98.38(7)	96.8(2)
Fe4−O2	2.004(2)	2.025(2)	Fe5−O3−Fe6	127.56(9)	126.6(3)
Fe4−O23	2.036(2)	2.017(2)	Fe5−O3−Fe4	120.94(8)	123.0(2)
Fe4−O3	1.946(2)	1.949(2)	Fe6−O3−Fe4	99.6(1)	98.8(2)
Fe5−O3	1.832(2)	1.833(2)	Fe6−O22−Fe1	98.79(8)	99.1(2)
Fe6−O2	2.029(2)	2.013(2)	Fe3−O23−Fe4	98.23(8)	99.5(2)
Fe6−O22	2.002(2)	1.958(2)			
Fe6−O3	1.925(2)	1.940(2)			

trends were observed around the μ_3-O^{2-} ions in the precursor complex $[Fe_4O_2(O_2CMe)_7(bpy)_2]^+$.

The two triangular units are also bridged by an acetate and a phenoxide group across each of the Fe2 pairs Fe1/Fe6 and Fe3/Fe4, and there is a unique acetate group bridging Fe3 and Fe6. As a result of the latter, the Fe3−O2−Fe6 angle [120.5(1)°] is much smaller than the Fe1−O2−Fe4 angle [153.8(1)°], which is the largest angle around O2. Each triangular unit has two carboxylate groups bridging one of its other Fe2 pairs and one carboxylate group bridging the third Fe2 pair. A chelating bpy ligand at each end of the cation completes the peripheral ligation, with all of the iron atoms exhibiting near-octahedral coordination geometry. Although there is no crystallographically imposed symmetry in the molecule, the cation has virtual C_2 symmetry, with the C_2 axis passing through the central μ_4-O^{2-} ion and the two carbon atoms of the central, unique carboxylate ligand.

The overall structure is very similar to that of $[Fe_6O_3(O_2CMe)_9(OEt)_2(bpy)_2](ClO_4)$,[15] with the main difference being the identity of the bridging alkoxide. As previously mentioned for the ethoxide complex, an analogy can be made between the core of **1** and that of the butterfly compound $[Fe_4O_2(O_2CMe)_7(bpy)_2](ClO_4)$[30] from which it derives: both
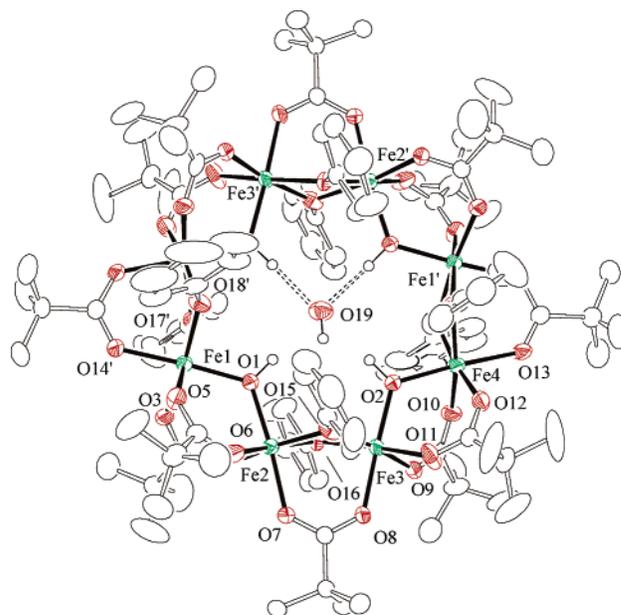
Figure 3. Labeled ORTEP representation of complex **2** at the 50% probability level. Hydrogen atoms, except for those involved in H bonds, have been omitted for clarity. Dashed lines are hydrogen bonds to the central H_2O molecule (O19). Primed and unprimed atoms are related by the inversion center.

compounds have similar trinuclear subunits with identical connectivity around the μ_3-oxide ligands, but whereas the two triangles are fused at one edge in the butterfly compound, in **1**, they are bridged by a μ_4-oxide ion. Consequently, there are four central or "body" iron ions in **1**, as opposed to two in the tetranuclear compound. Table 2 compares selected distances and angles for the cores of the cations of **1** and $[Fe_6O_3(O_2CMe)_9(OEt)_2(py)_2]^+$. It demonstrates that the core structures are nearly superimposable. The bulkier phenyl rings of **1** are perfectly accommodated in this structure without causing any kind of distortion compared to the ethoxide complex.

$[Fe_8(OH)_4(OPh)_8(O_2CBu^t)_{12}]\cdot H_2O\cdot CH_2Cl_2$ (**2**·H_2O·CH_2-Cl_2). An ORTEP representation of complex **2** is shown in Figure 3, and selected bond distances are listed in Table 3. The Fe_8 molecule lies on a center of symmetry, and thus, the asymmetric unit contains a half-molecule of Fe_8 and a half-molecule each of H_2O and CH_2Cl_2. The structure consists of a planar ring of eight Fe(III) ions, with the greatest deviation from the least-squares plane (0.029Å) being by Fe4. The Fe atoms are connected by two types of bridging groups, which alternate around the ring. Every iron ion is linked to one of its neighbors through a carboxylate group that is equatorial to the Fe_8 ring and two μ-phenoxo groups that are axial. The connection with the other neighboring Fe atom is through an equatorial μ-hydroxide group directed toward the center of the ring and two carboxylate groups, one above and one below the plane, with their *tert*-butyl groups directed outward. A molecule of water is disordered with equal occupancies between two positions in the center of the ring related by the inversion center,

(30) McCusker, J. K.; Vincent, J. B.; Schmitt, E. A.; Mino, M. L.; Shin, K.; Coggin, D. K.; Hagen, P. M.; Huffman, J. C.; Christou, G.; Hendrickson, D. N. *J. Am. Chem. Soc.* **1991**, *113*, 3012.
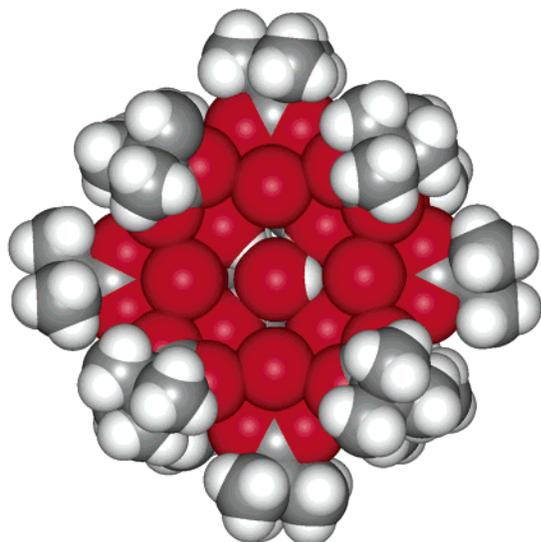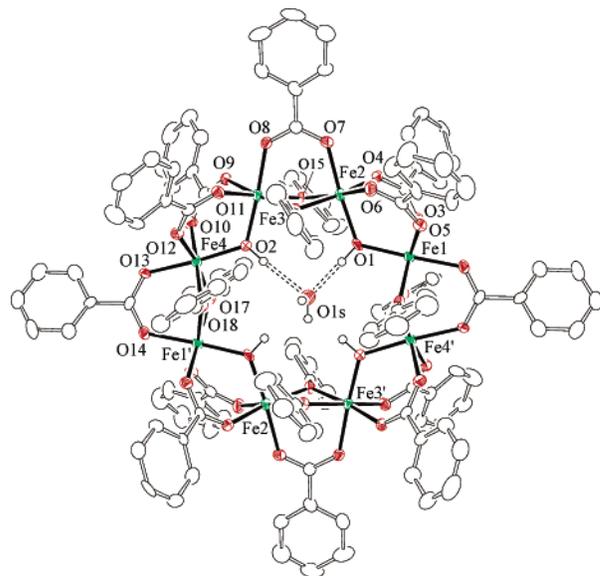
Figure 4. Space-filling representation of complex **2** perpendicular to the Fe8 plane, emphasizing the small size of the central cavity. Phenyl rings have been omitted for clarity.

Table 3. Selected Distances (Å) and Angles (deg) for Complex **2**·H_2O·CH_2Cl_2

Fe1−O1	1.982(2)	Fe3−O9	1.83(2)
Fe1−O5	1.983(2)	Fe3−O2	1.961(2)
Fe1−O3	1.991(2)	Fe3−O11	1.992(3)
Fe1−O18	2.007(2)	Fe3−O16	2.013(2)
Fe1−O17	2.017(2)	Fe3−O8	2.016(2)
Fe1−O14	2.028(2)	Fe3−O15	2.020(2)
Fe2−O1	1.981(2)	Fe4−O2	1.963(2)
Fe2−O6	1.983(2)	Fe4−O12	1.979(3)
Fe2−O4	1.984(2)	Fe4−O17	2.010(2)
Fe2−O15	2.007(2)	Fe4−O18	2.012(3)
Fe2−O16	2.015(2)	Fe4−O13	2.016(3)
Fe2−O7	2.024(2)	Fe4−O10	2.15(1)
O1···O19	3.081	O2···O19	2.991
Fe1−O1−Fe2	121.4(1)	Fe1′−O18−Fe4	100.7(1)
Fe2−O15−Fe3	100.6 (1)	Fe1′−O17−Fe4	100.4(1)
Fe2−O16−Fe3	100.55(9)	Fe3−O2−Fe4	120.7(1)
O1−H1···O19	170.94	O2−H2···O19	163.74

slightly above or slightly below the plane (0.569 Å). At each position, the water molecule forms hydrogen bonds with two hydroxide groups, as depicted by the dashed lines in Figure 3. Distances and angles relevant to these hydrogen bonds are included in Table 3. The water molecule in the alternative disorder position establishes hydrogen bonds with the two other hydroxide groups. The very tight fit of the water molecule in the center of the ring is evident from the space-filling view shown in Figure 4, which emphasizes the limited space in the center.

The structure of **2** is unprecedented in iron chemistry, although its metal/oxygen framework is related to that in the reported chromium(III) wheel ring compound [$Cr_8(OH)_{12}$-$(O_2CMe)_{12}$].[31] Only four other Fe8 wheel complexes have been reported to date, and their structures differ greatly from the one described here for **2**. Gerveleu et al.[32] synthesized the highly symmetrical wheel [$Fe_8F_8(O_2CBu^t)_{16}$], and Satcher et al.[33] reported the compound [$Fe_8O_4(BMDP)_4(OH)_4(O_2$-

(31) Eshel, M.; Bino, A.; Felner, I.; Johnston, D. C.; Luban, M.; Miller, L. L. *Inorg. Chem.* **2000**, *39*, 1376.
(32) Gerbeleu, N. V.; Stuchkov, Y. T.; Manole, O. S.; Timko, G. A.; Batsanov, A. S. *Dokl. Akad. Nauk SSSR* **1993**, *331*, 184.

Figure 5. Labeled ORTEP representation of complex **3** at the 50% probability level. Hydrogen atoms, except for those involved in hydrogen bonding, have been omitted for clarity. Dashed lines are hydrogen bonds to the central H_2O molecule (O1s). Primed and unprimed atoms are related by the inversion center.

$CMe)_4$]$^+$ (BMDP = *N,N,N′*-tris((*N*-methyl)-2-benzimida-zolylmethyl)-*N′*-methyl-1,3-diamino-2-propanoxide), which can best be described as an aggregation of dinuclear units bridged to each other through single μ_2-oxide groups and connected within each unit through an acetate group and the alkoxide group of the BMDP ligand. More recently, Jones and co-workers[34] prepared the nonplanar wheel complex [$Fe_8(O_2CPh)_{12}(thme)_4$] [$H_3thme$ = 1,1,1-tris(hydroxymethyl)-ethane]. Finally, Saalfrank et al.[35] synthesized the octanuclear metallacrown [Fe_8L_8] (LH_3 = triethanolamine), which encapsulates a Cs^+ cation as a guest. When the smaller cations Li^+ or Na^+ were employed in the same synthesis, a six-membered [Fe_6L_6] ring was formed instead, the size of the guest group clearly determining the dimension of the host ring. Our attempts to replace the central H_2O molecule with other small molecules or ions was directed toward the same objective, but attempts to accomplish this replacement to date have been unsuccessful.

$Fe_8(OH)_4(OPh)_8(O_2CPh)_{12}$·$H_2O$·3CHCl$_3$ (3·H_2O·3CH-Cl$_3$). An ORTEP representation of complex **3** is shown in Figure 5, and selected bond distances and angles are listed in Table 4. The overall structure of this complex is very similar to that of complex **2**. It consists of a planar ring arrangement of eight Fe atoms, with the greatest deviation from the least-squares plane (0.099 Å) being by Fe4. The metal ions are again connected by two alternating bridging systems: either a carboxylate and two phenoxide ligands or a μ_2-hydroxide and two carboxylate ligands. As for **2**, the Fe8 molecule of **3** lies on an inversion center. The major

(33) Satcher, J. H., Jr.; Olmstead, M. M.; Droege, M. W.; Parkin, S. R.; Noll, B. C.; May, L.; Balch, A. L. *Inorg. Chem.* **1998**, *37*, 6751.
(34) Jones, L. F.; Batsanov, A.; Brechin, E. K.; Collison, D.; Helliwell, M.; Mallah, T.; McInnes, E. J. L.; Piligkos, S. *Angew. Chem., Int. Ed.* **2002**, *41*, 4318.
(35) Saalfrank, R. W.; Bernt, I.; Uller, E.; Hampel, F. *Angew. Chem., Int. Ed. Engl.* **1997**, *36*, 2482.
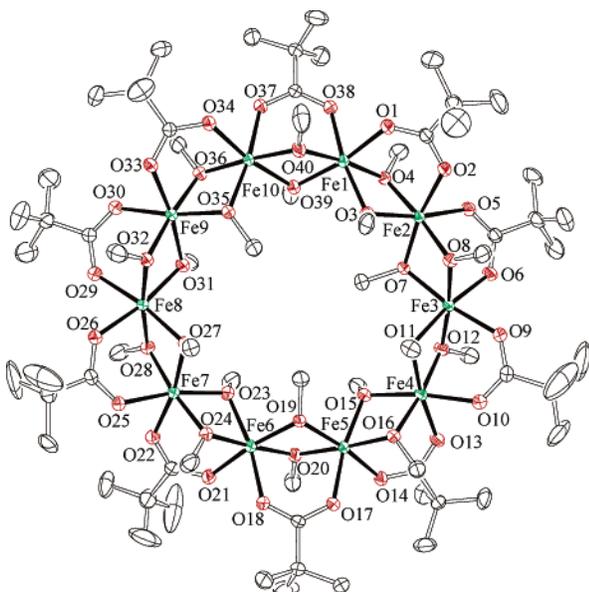
Figure 6. Labeled ORTEP representation of complex **4** at the 50% probability level. Hydrogen atoms have been omitted for clarity.

Table 4. Selected Distances (Å) and Angles (deg) for **3**·H$_2$O·3CHCl$_3$

Fe1−O1	1.975(6)	Fe3−O2	1.969(6)
Fe1−O3	1.995(6)	Fe3−O11	1.985(7)
Fe1−O5	2.006(6)	Fe3−O9	1.996(6)
Fe1−O18′	2.006(6)	Fe3−O16	2.013(6)
Fe1−O17′	2.031(6)	Fe3−O8	2.019(6)
Fe1−O14′	2.050(6)	Fe3−O15	2.026(7)
Fe2−O4	1.970(7)	Fe4−O12	1.964(7)
Fe2−O1	1.971(6)	Fe4−O2	1.976(6)
Fe2−O6	1.991(6)	Fe4−O10	2.004(7)
Fe2−O15	2.005(6)	Fe4−O17	2.009(6)
Fe2−O16	2.019(6)	Fe4−O13	2.019(6)
Fe2−O7	2.032(6)	Fe4−O18	2.022(6)
O1···O1s	2.97(2)	O2···O1s	3.08(2)
Fe1−O1−Fe2	121.9(3)	Fe3−O2−Fe4	121.4(3)
Fe2−O16−Fe3	100.4(3)	Fe1′−O17−Fe4	100.4(3)
Fe2−O15−Fe3	100.4(3)	Fe1′−O18−Fe4	100.8(3)
O1−H1···O1s	158.3	O2−H2···O1s	171.1

difference between the two compounds is the identity of the carboxylate: benzoate in **3** and pivalate in **2**. This difference has no major effect on the structural parameters of the core, and distances and angles relating the iron ions and their bridging groups are statistically the same in the two compounds. In addition to three molecules of CHCl$_3$ in the lattice, there is again a molecule of water held in the center of the Fe$_8$ ring by hydrogen bonds with two of the μ-OH$^-$ groups; pertinent distances and angles associated with the hydrogen bonds are included in Table 4. As in complex **2**, this water molecule is disordered between two symmetry-related positions, at 0.653 Å above and below the Fe$_8$ least-squares plane.

[Fe$_{10}$(OMe)$_{20}$(O$_2$CBu^t)$_{10}$]·CHCl$_3$ (4·CHCl$_3$). An ORTEP plot of complex **4** is shown in Figure 6, and selected bond distances and angles are listed in Table 5. The compound crystallizes in the triclinic space group $P\bar{1}$, with one Fe$_{10}$ cluster and one CHCl$_3$ molecule per unit cell. Its structure is very similar to that observed for the analogous compounds [Fe(OMe)$_2$(O$_2$CR)]$_{10}$ [R = CHPh$_2$,[26] Me,[27] CH$_2$Cl,[13] 3-(4-methylbenzoyl)-ethyl[29]], referred to as ferric wheels. It contains 10 octahedral Fe^{3+} atoms arranged in a planar ring.

Table 5. Selected Distances (Å) and Angles (deg) for [Fe$_{10}$(OMe)$_{20}$(O$_2$CBu^t)$_{10}$] (**4**)

Fe1−O4	1.984(2)	Fe6−O19	1.980(2)
Fe1−O39	1.987(2)	Fe6−O23	1.986(2)
Fe1−O40	1.987(2)	Fe6−O24	1.989(2)
Fe1−O3	1.996(2)	Fe6−O20	2.005(2)
Fe1−O38	2.029(2)	Fe6−O18	2.032(2)
Fe1−O1	2.037(2)	Fe6−O21	2.041(2)
Fe2−O4	1.983(2)	Fe7−O24	1.981(2)
Fe2−O3	1.984(2)	Fe7−O28	1.983(2)
Fe2−O8	1.998(2)	Fe7−O23	1.988(2)
Fe2−O7	2.002(2)	Fe7−O27	1.994(2)
Fe2−O5	2.025(2)	Fe7−O22	2.039(2)
Fe2−O2	2.039(2)	Fe7−O25	2.041(2)
Fe3−O11	1.986(2)	Fe8−O32	1.989(2)
Fe3−O12	1.992(2)	Fe8−O28	1.989(2)
Fe3−O7	1.994(2)	Fe8−O31	1.989(2)
Fe3−O8	1.996(2)	Fe8−O27	1.996(2)
Fe3−O9	2.031(2)	Fe8−O29	2.039(2)
Fe3−O6	2.037(2)	Fe8−O26	2.041(2)
Fe4−O12	1.983(2)	Fe9−O35	1.973(2)
Fe4−O16	1.987(2)	Fe9−O31	1.985(2)
Fe4−O15	1.988(2)	Fe9−O32	1.992(2)
Fe4−O11	1.991(2)	Fe9−O36	2.000(2)
Fe4−O10	2.044(2)	Fe9−O30	2.041(2)
Fe4−O13	2.046(2)	Fe9−O33	2.045(2)
Fe5−O19	1.973(2)	Fe10−O35	1.976(2)
Fe5−O15	1.989(2)	Fe10−O39	1.985(2)
Fe5−O20	1.997(2)	Fe10−O40	1.989(2)
Fe5−O16	2.000(2)	Fe10−O36	2.002(2)
Fe5−O17	2.034(2)	Fe10−O34	2.034(2)
Fe5−O14	2.046(2)	Fe10−O37	2.050(2)
Fe2−O3−Fe1	98.78(8)	Fe6−O23−Fe7	99.16(8)
Fe2−O4−Fe1	99.24(8)	Fe7−O24−Fe6	99.33(9)
Fe3−O7−Fe2	98.19(8)	Fe7−O27−Fe8	98.27(8)
Fe3−O8−Fe2	98.23(8)	Fe7−O28−Fe8	98.87(9)
Fe3−O11−Fe4	98.88(8)	Fe9−O31−Fe8	99.10(8)
Fe4−O12−Fe3	98.96(8)	Fe8−O32−Fe9	98.89(9)
Fe4−O15−Fe5	98.89(8)	Fe9−O35−Fe10	99.49(8)
Fe4−O16−Fe5	98.54(8)	Fe9−O36−Fe10	97.70(9)
Fe5−O19−Fe6	99.37(8)	Fe10−O39−Fe1	99.14(8)
Fe5−O20−Fe6	97.75(8)	Fe1−O40−Fe10	98.97(9)

Every Fe atom is linked to the neighboring metals through two μ_2-methoxide and one μ_2-carboxylate bridges. Although the complex does not have any crystallographic symmetry, it exhibits virtual D_{5d} symmetry. The carboxylate ligands are alternately disposed above and below the Fe$_{10}$ plane. Similarly, the methoxide groups are alternately directed either toward the center or toward the periphery of the molecule. The Fe−O−Fe angles are statistically equivalent, 98.8(5)°, as are the Fe−O bond lengths along these bridges, 1.989(9) Å. The distances between the iron ions and the oxygen atoms from the carboxylate groups are slightly longer, 2.04(1) Å. The *tert*-butyl groups of the carboxylate are randomly oriented, which constitutes the major disruption of the symmetry of the complex.

Magnetochemistry. DC magnetic susceptibility data for complexes **2** and **4** were collected in a 1-T applied field in the temperature range 2.0−300 K. [Fe$_6$O$_3$(O$_2$CMe)$_9$(OPh)$_2$-(bpy)$_2$](ClO$_4$) (**1**) is expected to have magnetic properties very similar to those of the previously studied ethoxide complex,[15] and data were thus not collected. Similarly, data were not collected on complex **3**, which is expected to be magnetically very similar to **2**.

[Fe$_8$(OH)$_4$(OPh)$_8$(O$_2$CBu^t)$_{12}$] (2). A plot of the effective magnetic moment (μ_{eff} per Fe$_8$) vs temperature is displayed in Figure 7. The μ_{eff} value decreases gradually from 13.19
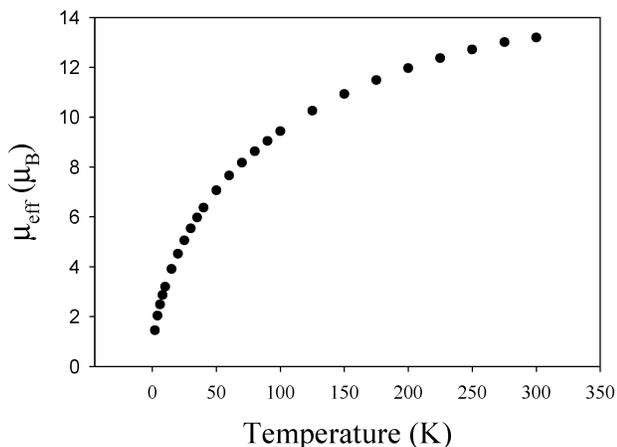
Figure 7. Plot of the effective magnetic moment (μ_{eff}/Fe₈) vs T for complex **2**.

μ_B at 300 K to 1.45 μ_B at 2.0 K. μ_{eff} at 300 K is below the spin-only ($g = 2$) value calculated for eight noninteracting Fe(III) ions (16.7 μ_B), which indicates the presence of antiferromagnetic exchange interactions in **2**. The overall profile of the curve is characteristic of a spin-singlet ($S = 0$) ground state with $S > 0$ excited states that are thermally populated in the 2.0–300 K range. A spin-singlet ground state is consistent with, and expected for, the topology of the compound, a ring of eight high-spin Fe(III) ions ($S_i = \frac{5}{2}$; $i = 1-8$), each expected to exhibit antiferromagnetic exchange interactions with its nearest neighbors. In this arrangement, there is no spin frustration arising from competing exchange interactions. On the contrary, the individual spins of each metal center alternate between parallel (spin-up) and antiparallel (spin-down) alignments, satisfying all of the antiferromagnetic interactions between vicinal Fe atoms.

Complex **2** displays approximate 4-fold symmetry, and this greatly simplifies the Heisenberg spin Hamiltonian describing the exchange interactions in the system. Only two kinds of interaction are needed in 4-fold symmetry: J_a, the interaction between two Fe atoms bridged by a μ-OH⁻ and two carboxylate groups, and J_b, the interaction between two Fe atoms bridged by two μ-phenoxide and one carboxylate groups. The resulting spin Hamiltonian is given by

$$\mathcal{H} = -2J_a[\hat{S}_1 \cdot \hat{S}_2 + \hat{S}_3 \cdot \hat{S}_4 + \hat{S}_{1A} \cdot \hat{S}_{2A} + \hat{S}_{3A} \cdot \hat{S}_{4A}] - 2J_b[\hat{S}_2 \cdot \hat{S}_3 + \hat{S}_4 \cdot \hat{S}_{1A} + \hat{S}_{2A} \cdot \hat{S}_{3A} + \hat{S}_{4A} \cdot \hat{S}_1] \quad (4)$$

Despite the high symmetry and relative simplicity of this system, it is not possible to apply the Kambe[36] method to derive an equivalent operator expression for the spin Hamiltonian that would allow straightforward derivation of its eigenvalues. However, we did carry out semiempirical calculations that proved extremely valuable in providing relevant information about the magnetic behavior of this compound. We employed the recently developed ZILSH method (derived from a combination of the ZINDO method, Davidson's local spin method, and the Heisenberg spin model),[24] which uses semiempirical molecular orbital cal-

(36) Kambe, K. *J. Phys. Soc. Jpn.* **1950**, *5*, 48.

Table 6. ZILSH Exchange Parameters (J_{AB}) between Iron Atoms in Complex **2**

A	B	J_{AB} (cm⁻¹)
1	2	−19.2
2	3	−14.4
3	4	−21.5
4	1′	−9.8

culations to provide estimates of two important quantities: (i) the exchange interaction parameter (J_{AB}) between each pair of interacting centers A and B and (ii) the average value of the spin couplings, $\hat{S}_A \cdot \hat{S}_B$. The two values provide complementary information about the system: J_{AB} indicates the preferred alignment of spins S_A and S_B, whereas $\hat{S}_A \cdot \hat{S}_B$ reflects the actual alignment of the spins, with a positive value if they are aligned parallel and a negative value if they are aligned antiparallel. The exchange parameters obtained from these ZILSH calculations on complex **2** are listed in Table 6. The ZILSH method makes no approximations regarding the symmetry of the molecule, nor does it neglect any magnetic interaction. The calculated values for exchange interactions between nonadjacent Fe atoms in the cluster were found to be approximately zero. As can be seen in Table 6, the rest of the interactions are all antiferromagnetic (J negative) and can be grouped into two pairs: J_{12} and J_{34} correspond to J_a in the Hamiltonian of eq 4, whereas J_{23} and $J_{4'A}$ correspond to J_b. The interactions (J_a) through a single μ-hydroxide group are on average −20.4 cm⁻¹, almost a factor of 2 stronger than those (J_b) between Fe atoms bridged by two μ-phenoxide groups, −12.1 cm⁻¹. These observations are in agreement with recently reported results from a magnetostructural correlation for diverse polynuclear high-spin Fe(III) compounds. The correlation revealed that the exchange interaction is more strongly antiferromagnetic when the Fe−O−Fe angle increases and the Fe−O bond distance decreases. In complex **2**, the average Fe−O−Fe angle through the single μ-hydroxide ion is 121°, considerably larger than the average angle through the oxygen atom of the phenoxide groups, 100.6°. Likewise, the mean Fe−O distance through the hydroxide bond is 1.97 Å, significantly shorter than the average bond distance through the phenoxide bridge, 2.01 Å.

The spin coupling values in a singlet spin component of the complex, $\hat{S}_A \cdot \hat{S}_B$, are presented schematically in Figure 8. This value was calculated to be negative for every pair of adjacent Fe atoms, corresponding to spins that are aligned antiparallel, whereas it is positive for interactions between every other metal. Block arrows in Figure 8 depict the spin alignments in this scheme, but it must be remembered that the assignment of a spin moment to each metal in an overall singlet spin state, represented by an arrow pointing up or down, is intuitive and useful but not rigorously correct. The average z component of the spin of each metal is zero in a spin-singlet ground state. The schematic depiction of spin using arrows in Figure 8 represents only one of the leading contributions to the wave function of the ground state, rather than a unique depiction of the ground state. Other contributions exist with reversed spin alignments that result in a net z component of spin of zero at each metal center. It is for

approximately 4.4 unpaired electrons reside on each iron atom, with the rest of the spin delocalized onto the ligands. This is similar to results obtained for other Fe^{3+} complexes with ZILSH[24,25] and DFT[39] calculations.

Conclusions

The results presented in this work further illustrate the value of alcoholysis reactions as a means to induce the aggregation of small clusters into compounds of larger nuclearity. In addition, we have extended such alcoholysis reactions to phenol for the first time, and our initial results with the latter suggest that a rich new source of high nuclearity products might await discovery. Four new compounds have been reported in this work. $[Fe_6O_3(O_2CMe)_9(OPh)_2(bpy)_2](ClO_4)$ has been obtained by treatment of $[Fe_4O_2(O_2CMe)_7(bpy)_2](ClO_4)$ with PhOH, in a reaction analogous to one that we reported previously for the ethoxide analogue. This pair of reactions indicates that, for this particular reaction system at least, the identity of the alkoxide does not influence the outcome of the reaction. In contrast, the product of the alcoholysis of the hexanuclear compound $[Fe_6O_2(OH)_2(O_2CBu^t)_{10}(hep)_2]$ is clearly determined by the size of the alcohol reagent: treatment with MeOH afforded the decanuclear compound $[Fe_{10}(OMe)_{20}(O_2CBu^t)_{10}]$, whereas a similar reaction with PhOH produced $[Fe_8(OH)_4(OPh)_8(O_2CBu^t)_{12}]$, a cluster with a new type of eight-membered ring structure. The benzoate analogue, $[Fe_8(OH)_4(OPh)_8(O_2CPh)_{12}]$, can also be prepared in a similar fashion. The formation of different products with phenol compared with MeOH can readily be rationalized on the basis of the structure of the Fe_{10} product and the clear impossibility of its accommodating bulkier phenoxide groups. Aside from its unquestionable aesthetic appeal, this Fe_8 molecule is also attractive because it contains a water molecule as a guest in its center. It might thus be possible to synthesize other ring complexes with different guest groups and perhaps different nuclearities, but preliminary attempts in this direction have been unsuccessful. Clearly, more forcing conditions or a better choice of alternative guest are required, and additional attempts are in progress. It is also of interest to explore reactions with even bulkier alkoxide groups. These and other studies in the alcoholysis and phenolysis of metal clusters are in progress.

The magnetic properties of the wheel compounds $[Fe_{10}(OMe)_{20}(O_2CBu^t)_{10}]$ and $[Fe_8(OH)_4(OPh)_8(O_2CBu^t)_{12}]$ have been studied by DC susceptibility measurements, and the exchange parameters gauging the interactions between metal centers have been calculated using the recently developed ZILSH computational method, which makes no approximations regarding symmetry. This method generally provides a qualitatively accurate description of magnetic interactions and correctly predicts the ground-state spin in Fe(III) complexes. Taken together, the computational and DC susceptibility results provide a clear picture of the magnetic interactions in both compounds: antiferromagnetic interactions between contiguous iron atoms result in antiparallel alignments of the spins and, consequently, spin-singlet ground states. Although the results for these two complexes are as expected, the present work further emphasizes the utility of the ZILSH method, which is proving itself to be an extremely important tool for the study of exchange-coupled polynuclear metal clusters.

Supporting Information Available: X-ray crystallographic files in CIF format for complexes **1**·2MeCN·PhOH, **2**·H_2O·CH_2Cl_2, **3**·H_2O·3CHCl₃, and **4**·CHCl₃. This material is available free of charge via the Internet at http://pubs.acs.org.

(39) Zeng, Z.; Duan, Y.; Guenzburger, D. *Phys. Rev. B* **1997**, *55*, 12522.

IC034706G